




## Weighing single-lined spectroscopic binaries using tidal RVs: the case of V723 Mon

K. Masuda<sup>1</sup>, T. Hirano<sup>2,3</sup> and M. Tomoyoshi<sup>1</sup>

<sup>1</sup> *Department of Earth and Space Science, Osaka University, Osaka  
560-0043, Japan (E-mail: kmasuda@ess.sci.osaka-u.ac.jp)*

<sup>2</sup> *Astrobiology Center, NINS, 2-21-1 Osawa, Mitaka, Tokyo 181-8588, Japan*

<sup>3</sup> *National Astronomical Observatory of Japan, NINS, 2-21-1 Osawa, Mitaka,  
Tokyo 181-8588, Japan*

Received: November 2, 2024; Accepted: December 10, 2024

**Abstract.** The tidal deformation of a star in a close binary not only produces the photometric flux variations (ellipsoidal variations, ELVs) but also causes the apparent radial velocity (RV) variations due to asymmetric distortion of the absorption lines. This “tidal RV” signal contains information equivalent to that from photometric ELVs, enabling its use in mass estimation for single-lined spectroscopic binaries (SB1s) and offering a potentially more robust approach against contaminating light relative to ELVs. In this work, we develop a quantitative model for the tidal RV signal and apply it to the binary system V723 Monocerotis, where both ELV and tidal RV signals are detected, and successfully determine the component masses using only the primary star’s absorption lines. The masses derived from the tidal RV modeling show a reasonable agreement with those from an analysis based on ELVs that carefully accounts for the flux contamination from the secondary star. This result demonstrates that tidal RVs provide a useful alternative means for mass estimation in SB1s.

**Key words:** Radial velocity – Red giant stars – Tidal distortion

### 1. Introduction

Many important binary systems are observed as single-lined spectroscopic binaries (SB1s). In a tight SB1 that exhibits flux variations due to tidal deformation of the primary star (ellipsoidal variations, ELVs),<sup>1</sup> the binary mass can be determined by combining ELVs with the primary’s radial velocity (RV) variations due to orbital motion and information of the primary’s radius. This method has been used for the mass estimation in close binaries including X-ray systems, but it has been pointed out that contaminating light from sources other than the primary star, if not properly taken into account, can introduce systematic errors in the mass and inclination estimates (Kreidberg et al., 2012).

<sup>1</sup>In this work, the “primary” refers to the brighter component of an SB1 for which radial velocities are measured, and it is not necessarily more massive than the secondary.

In this work, we focus on spectroscopic effects of tidal deformation as an alternative means for binary mass estimation. The deformation of the primary star does not only change the apparent size of the star, it also changes the relative area of the approaching and receding parts of the visible stellar surface in phase with the orbit. This results in asymmetric distortion of the Doppler-broadened absorption lines, and induces apparent RV variations (e.g., [Sterne, 1941](#); [Kopal, 1959](#)); see Figure 1. Because this “tidal RV” signal shares a common origin as ELVs, it should in principle enable mass estimation of an SB1 system using only the primary star’s absorption lines from high-resolution spectroscopic data, providing a potentially more robust approach against flux contamination that reduces the photometric ELV amplitude. To test this concept, we develop a quantitative model of the tidal RV signal and apply it to the binary system V723 Monocerotis. The system consists of a red giant primary and a more compact, hotter subgiant secondary ([El-Badry et al., 2022](#)), where significant tidal deformation of the primary has enabled detection of both EVs and tidal RV signals ([Jayasinghe et al., 2021](#); [Masuda & Hirano, 2021](#)).

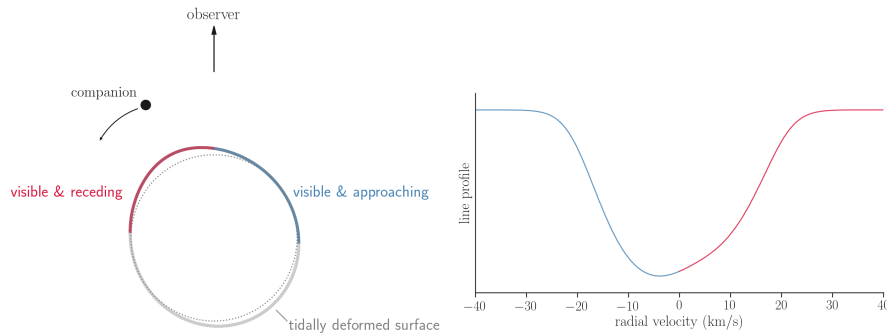


**Figure 1.** Schematic illustration of the tidal effect on the absorption line profile; figure from [Masuda & Hirano \(2021\)](#). (*Left*)— The thick gray line shows the equator of the red giant deformed by the companion. (*Right*)— The absorption line profile corresponding to the configuration shown in the left panel.

## 2. The tidal RV model

We model the RV signal due to the orbital motion and tidal deformation effects in the following steps. See [Masuda & Hirano \(2021\)](#) for more details.

1. The distributions of the flux and line-of-sight velocity over the surface of the primary star is computed adopting the Roche model, given the time of inferior conjunction (secondary star is in front)  $t_0$ , orbital period  $P$ , inclination  $i$ , primary’s mass  $M_1$ , secondary’s mass  $M_2$ , primary’s radius  $R_1$ , gravity-darkening coefficient  $y$ , and two limb-darkening coefficients  $u_1$

and  $u_2$  for the quadratic law. The flux and velocity values are evaluated at 768 `HEALPix`/`healpy` pixels (Górski et al., 2005). The gravity- and limb-darkening coefficients are constrained to be around the values determined as a function of a single effective wavelength  $\lambda_{\text{eff}}$  using the relation in Claret & Bloemen (2011).

2. The flux and velocity distributions are used to compute the absorption line profile of the primary star, given the macroturbulence velocity  $\zeta$ . For the macroturbulence velocity field, we adopt a radial-tangential model and assume the common velocity dispersions for both directions.
3. The line profile model was used to simulate the cross-correlation function (CCF) as results from cross-correlating the observed spectrum with a theoretical template spectrum, whose line profile is assumed to be a Gaussian with the standard deviation (in the velocity space) of  $\beta$ . The tidal RV,  $v_{\text{tidal}}$ , is computed as the velocity corresponding to the CCF peak.
4. The center-of-mass velocities  $v_0$  of the primary star due to orbital motion are computed as  $v_0(t) = -K \sin \left[ \frac{2\pi(t-t_0)}{P} \right] + \gamma$ , where  $K$  is computed from the above  $M_1$ ,  $M_2$ ,  $i$ , and  $P$ , and  $\gamma$  is the RV zero point. Then the full physical model for the observed RVs is  $v_{\text{model}}(t) = v_0(t) + v_{\text{tidal}}(t)$ .

The above physical RV model is specified by the set of parameters  $\theta = \{M_1, M_2, R_1, t_0, P, i, \zeta, \lambda_{\text{eff}}, \beta, \gamma\}$ , which are inferred from the RV data simultaneously.

### 3. Application to V723 Mon

We use the model in the previous section to fit the RV data of V723 Mon from Strassmeier et al. (2012). The velocities were derived from high-resolution ( $R = 55,000$ ), optical (338–882 nm) spectra from the STELLA échelle spectrograph (SES) on the 1.2 m STELLA-I telescope at the Teide Observatory (Strassmeier et al., 2004; Weber et al., 2008; Strassmeier et al., 2010), via a cross correlation analysis using a synthetic spectrum. We also adopt  $v \sin i = 15.7 \pm 1.0$  km/s and  $\zeta = 2.0 \pm 1.1$  km/s determined by forward-modeling the Subaru/IRD spectrum of this target as additional constraints; see Tomoyoshi et al. (2024) for details.

Figure 2 shows the inferred RV model along with the observed data. We successfully modeled the tidal RV signal (upper-middle panel), and obtained  $M_1 = 0.46^{+0.12}_{-0.09} M_{\odot}$  and  $M_2 = 2.5 \pm 0.2 M_{\odot}$  using spectroscopic information (i.e., RVs and line widths) alone. Although we did not explicitly take into account the significant contamination of the secondary’s flux in this system (El-Badry et al., 2022), our results show a reasonable agreement with  $M_1 = 0.44 \pm 0.06 M_{\odot}$  and  $M_2 = 2.8 \pm 0.3 M_{\odot}$  obtained from the absolute flux and ELVs, after carefully modeling the secondary’s flux contamination (El-Badry et al., 2022).

This serves as a proof of concept that modeling of tidal RVs is useful as an alternative means to measure the mass of tidally deformed SB1s. As shown in

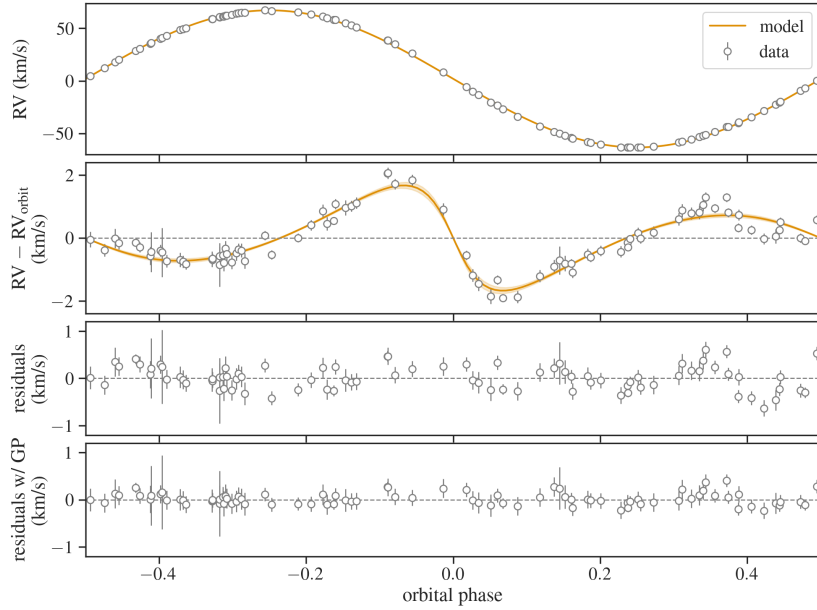


**Figure 2.** The observed and modeled RVs as a function of orbital phase. The white filled circles are the RV data from [Strassmeier et al. \(2012\)](#). The orange solid line and the shaded region respectively show the mean and standard deviation of the posterior models. (*Top*) — Raw RVs. (*Upper-middle*) — RVs relative to the orbital component plus  $\gamma$  ( $v_{\text{tidal}}$  in Section 2). (*Lower-middle*) — Residuals relative to the full physical model. (*Bottom*) — RVs relative to the full physical model + mean prediction of the Gaussian process noise model.

the corner plot for  $M_1$ ,  $M_2$ ,  $R_1$ , and  $i$  (Figure 3), however, our modeling (black contours) prefers  $\sim 2\sigma$  larger  $i$  and smaller  $R_1$  than those derived by [El-Badry et al. \(2022\)](#) (red crosses) so that the resulting  $v \sin i$  remains similar. This could indicate a systematic error in the inclination estimate in our tidal RV modeling. If this bias is indeed present, one possible explanation is that our analytic CCF evaluation model may be overly simplified, as it assumes a uniform shape for all absorption lines. Reducing this type of systematic error may be possible by directly modeling the line shapes rather than using RV values derived from distorted lines. This approach will be explored in future work.

#### 4. Summary and conclusion

We developed a quantitative model for the apparent RV variations due to orbital-phase-dependent tidal deformation of a star, and used it to determine the physical parameters of the binary system V723 Mon only using RVs and

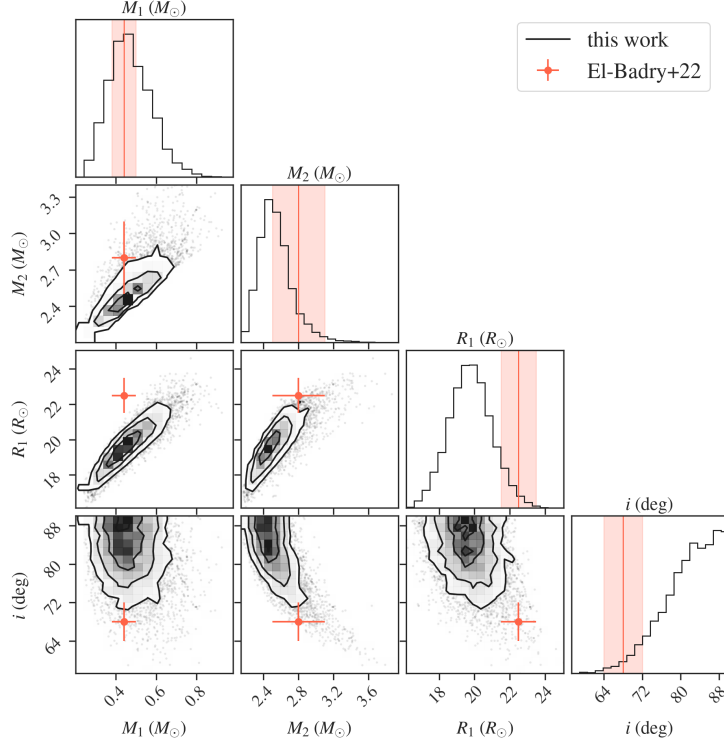


**Figure 3.** Corner plot for the posterior samples obtained from our tidal RV modeling (black contours and histograms). The red crosses are the values derived by [El-Badry et al. \(2022\)](#) using ELVs.

$v \sin i$  of the primary star. To our knowledge, this is the first quantitative mass measurement of an SB1 system using only spectroscopic data, independent of stellar models or absolute flux information. Although we did not explicitly model the secondary’s significant flux, the masses derived ( $M_1 = 0.46^{+0.12}_{-0.09} M_\odot$  and  $M_2 = 2.5 \pm 0.2 M_\odot$ ) align well with those from ellipsoidal variations ( $M_1 = 0.44 \pm 0.06 M_\odot$  and  $M_2 = 2.8 \pm 0.3 M_\odot$ ) and SED analysis that fully takes into account the significant secondary’s flux ([El-Badry et al., 2022](#)). This demonstrates that tidal RV modeling offers a potentially useful alternative for mass measurements of tidally deformed SB1s of particular interest, such as X-ray faint, dormant compact object binaries that are being uncovered from ongoing large surveys. Comparing ELV- and tidal-RV-based results also reveals a possible inclination biases in tidal RV modeling, which may be mitigated by directly modeling phase-dependent line distortions. This is a task for future work.

**Acknowledgements.** The authors are grateful to the organizers of the conference “Binary and Multiple Stars in the Era of Big Sky Surveys.” K.M. acknowledges support

by JSPS KAKENHI grant No. 21H04998.

## References

- Claret, A. & Bloemen, S., Gravity and limb-darkening coefficients for the Kepler, CoRoT, Spitzer, uvby, UBVRIJHK, and Sloan photometric systems. 2011, *Astronomy and Astrophysics*, **529**, A75, DOI:10.1051/0004-6361/201116451
- El-Badry, K., Seeburger, R., Jayasinghe, T., et al., Unicorns and giraffes in the binary zoo: stripped giants with subgiant companions. 2022, *Monthly Notices of the RAS*, **512**, 5620, DOI:10.1093/mnras/stac815
- Górski, K. M., Hivon, E., Banday, A. J., et al., HEALPix: A Framework for High-Resolution Discretization and Fast Analysis of Data Distributed on the Sphere. 2005, *Astrophysical Journal*, **622**, 759, DOI:10.1086/427976
- Jayasinghe, T., Stanek, K. Z., Thompson, T. A., et al., A unicorn in monoceros: the 3  $M_{\odot}$  dark companion to the bright, nearby red giant V723 Mon is a non-interacting, mass-gap black hole candidate. 2021, *Monthly Notices of the RAS*, **504**, 2577, DOI:10.1093/mnras/stab907
- Kopal, Z. 1959, *Close binary systems*
- Kreidberg, L., Bailyn, C. D., Farr, W. M., & Kalogera, V., Mass Measurements of Black Holes in X-Ray Transients: Is There a Mass Gap? 2012, *Astrophysical Journal*, **757**, 36, DOI:10.1088/0004-637X/757/1/36
- Masuda, K. & Hirano, T., Tidal Effects on the Radial Velocities of V723 Mon: Additional Evidence for a Dark 3  $M_{\odot}$  Companion. 2021, *Astrophysical Journal, Letters*, **910**, L17, DOI:10.3847/2041-8213/abecdc
- Sterne, T. E., Notes on Binary Stars. IV. A Source of Spurious Eccentricity in Spectroscopic Binaries. 1941, *Proceedings of the National Academy of Science*, **27**, 168, DOI:10.1073/pnas.27.3.168
- Strassmeier, K. G., Granzer, T., Weber, M., et al., The STELLA robotic observatory. 2004, *Astronomische Nachrichten*, **325**, 527, DOI:10.1002/asna.200410273
- Strassmeier, K. G., Granzer, T., Weber, M., et al., The STELLA Robotic Observatory on Tenerife. 2010, *Advances in Astronomy*, **2010**, 970306, DOI:10.1155/2010/970306
- Strassmeier, K. G., Weber, M., Granzer, T., & Järvinen, S., Rotation, activity, and lithium abundance in cool binary stars. 2012, *Astronomische Nachrichten*, **333**, 663, DOI:10.1002/asna.201211719
- Tomoyoshi, M., Masuda, K., Hirano, T., et al., Weighing Single-lined Spectroscopic Binaries Using Tidal Effects on Radial Velocities: The Case of V723 Monocerotis. 2024, *arXiv e-prints*, arXiv:2410.22083, DOI:10.48550/arXiv.2410.22083
- Weber, M., Granzer, T., Strassmeier, K. G., & Woche, M., The STELLA robotic observatory: first two years of high-resolution spectroscopy. 2008, in Society of Photo-Optical Instrumentation Engineers (SPIE) Conference Series, Vol. **7019**, *Advanced Software and Control for Astronomy II*, ed. A. Bridger & N. M. Radziwill, 70190L